

General Disclaimer

One or more of the Following Statements may affect this Document

- This document has been reproduced from the best copy furnished by the organizational source. It is being released in the interest of making available as much information as possible.
- This document may contain data, which exceeds the sheet parameters. It was furnished in this condition by the organizational source and is the best copy available.
- This document may contain tone-on-tone or color graphs, charts and/or pictures, which have been reproduced in black and white.
- This document is paginated as submitted by the original source.
- Portions of this document are not fully legible due to the historical nature of some of the material. However, it is the best reproduction available from the original submission.

[illegible]

INTERIM REPORT ON MICROFISSURING OF INCONEL 718

N83-29356

G3/26 Unclass
12958

June 1983

*Registered trademark of the Inco family of companies.



George C. Marshall Space Flight Center

TECHNICAL REPORT STANDARD TITLE PAGE					
1. REPORT NO. NASA TM-82531		2. GOVERNMENT ACCESSION NO.		3. RECIPIENT'S CATALOG NO.	
4. TITLE AND SUBTITLE Interim Report on Microfissuring of Inconel 718				5. REPORT DATE June 1983	
				6. PERFORMING ORGANIZATION CODE	
7. AUTHOR(S) A. C. Nunes, Jr.				8. PERFORMING ORGANIZATION REPORT #	
9. PERFORMING ORGANIZATION NAME AND ADDRESS George C. Marshall Space Flight Center Marshall Space Flight Center, Alabama 35812				10. WORK UNIT NO.	
				11. CONTRACT OR GRANT NO.	
12. SPONSORING AGENCY NAME AND ADDRESS National Aeronautics and Space Administration Washington, DC 20546				13. TYPE OF REPORT & PERIOD COVERED Technical Memorandum	
				14. SPONSORING AGENCY CODE	
15. SUPPLEMENTARY NOTES Prepared by Materials and Processes Laboratory, Science and Engineering Directorate.					
16. ABSTRACT A tentative mathematical computer model of the microfissuring process during electron beam welding of Inconel 718 has been constructed. Predictions of the model are compatible with microfissuring tests on eight 0.25-in. thick test plates. The model takes into account weld power and speed, weld loss (efficiency), parameters and material characteristics. Besides the usual material characteristics (thermal and strength properties), a temperature and grain size dependent critical fracture strain is required by the model. The model is based upon fundamental physical theory (i.e., it is not a mere data interpolation system), and can be extended to other metals by suitable parameter changes. <div style="text-align: center;">ORIGINAL PAGE IS OF POOR QUALITY</div>					
17. KEY WORDS Microfissure Inconel 718 Mathematical computer model Electron beam welding Material characteristics			18. DISTRIBUTION STATEMENT Unclassified-Unlimited		
19. SECURITY CLASSIF. (of this report)		20. SECURITY CLASSIF. (of this page)		21. NO. OF PAGES	
Unclassified		Unclassified		27	
				22. PRICE NTIS	

ACKNOWLEDGMENTS

The author wishes to express his appreciation for special assistance provided by NASA co-workers. The problem was originally suggested by M. C. McIlwain. S. T. Webster operated the EB welder. W. R. DeWeese etched the specimens. E. R. Risch provided dye penetrant tests. J. R. Williams, Chief of the Test Laboratory Fabrication Division, provided initial machining and heat treatment of the weld specimens. B. N. Bhat of the Metallurgy Research Branch and C. J. Bianca of the Engineering Analysis Division read the report and made some good suggestions. R. R. Rowe and J. H. Hess of the Metallurgy Research Branch also contributed advice on testing to be carried out and reported on at a later time.

Other contributors outside of NASA were R. G. Thompson, who spent two summers at MSFC studying microfissuring and is currently continuing microfissuring research at the University of Alabama in Birmingham, and Glenn Engineering Co., Inc., of Huntsville, Alabama, which provided surface grinding used to uncover microfissured material.

W. A. Wilson, the author's Branch Chief, must be cited for his active encouragement of the effort.

It is possible that with so many contributors a significant contributor could have been neglected. To leave room for this possibility the list should not be regarded as necessarily complete.

TABLE OF CONTENTS

	Page
INTRODUCTION	1
TEST PROCEDURE	2
TEST RESULTS	4
THEORY OF MICROFISSURING	4
COMPARISON OF THEORY AND EXPERIMENT	11
CONCLUSIONS AND RECOMMENDATIONS	13
REFERENCES	14
APPENDIX A - MICROFISSURING MODEL COMPUTER PROGRAM LISTING	15
APPENDIX B - SAMPLE MICROFISSURING MODEL OUTPUT'	21

LIST OF ILLUSTRATIONS

Figure	Title	Page
1.	Grain growth in Inconel 718 during 1 hr exposure to various temperatures followed by air cool to room temperature	2
2.	Crown and root widths of EB welds in 0.25-in. thick Inconel 718 plate made with the same energy per unit weld length but at different weld speed/power combinations. Focus adjustments needed to maintain approximately the same crown and root width are also shown	3
3.	Microfissures per inch versus beam power and approximate location of microfissuring envelope point on speed/power constant weld cross section line	5
4.	Overall and nailhead power losses versus weld speed for constant energy per length equivalent profile EB welds	7
5.	Microfissures per inch versus microfissuring power excess	12
6.	Computer output: weld speed versus beam power	21
7.	Computer output: damage versus beam power	22
8.	Computer output: weld speed versus damage	22

LIST OF TABLES

Table	Title	Page
1.	Welding Parameters Used	3
2.	Computer Model Predictions of Power-Speed Combination at Which Microfissuring Begins	11
3.	Excess Power Above Computer Model Power Requirement to Initiate Microfissuring	12

TECHNICAL MEMORANDUM

INTERIM REPORT ON MICROFISSURING OF INCONEL 718

INTRODUCTION

When Inconel 718, a major constituent of the Space Shuttle Main Engine, is welded, microfissures are often found between the grains of the metal in the heat-affected zone (HAZ) of the weld. Microfissures were discovered in Inconel 718 in 1965 [1]. Since that time a great amount of effort devoted to studying the metallographical setting in which microfissuring occurs failed to yield an understanding adequate to control it, so attention was turned toward the dynamics of the microfissuring process itself [2].

In 1976 [3], Professor Y. Arata and a team of Japanese researchers from Kawasaki Heavy Industries, Ltd., published microfissuring envelopes separating regions of higher weld speed/electron beam (EB) power settings at which microfissuring was encountered in EB welds from lower speed/power settings at which microfissuring did not occur. They covered speeds to 60 inches per minute (IPM) and powers to 7 kW. Microfissuring envelopes for Hastelloy X in several heat treat conditions, as well as for Incoloy 800 and Incoloy 901, were plotted.

The microfissuring envelopes of Arata et al. comprise a potentially very useful tool not only for eliminating microfissuring through adjustment of processing parameters but for characterizing the microfissuring tendency of a particular metal as well.

Microfissuring appears to be associated with grain boundary liquation [4,5] below the solidus temperature, but microfissuring does not necessarily occur when grain boundary liquation is present [6]. This implies that grain boundary liquation can set up a condition of brittle vulnerability at temperatures slightly below the alloy solidus, but a second condition, sufficient mechanical strain, must also be met before microfissures form. Cracks tend to open up in a direction perpendicular to the maximum tensile strain. A study of the orientation of microfissures [7] suggests that the strains responsible for microfissuring are oriented in a direction perpendicular to the plane of the workpiece surface or (often the same thing) parallel to the weld puddle boundary.

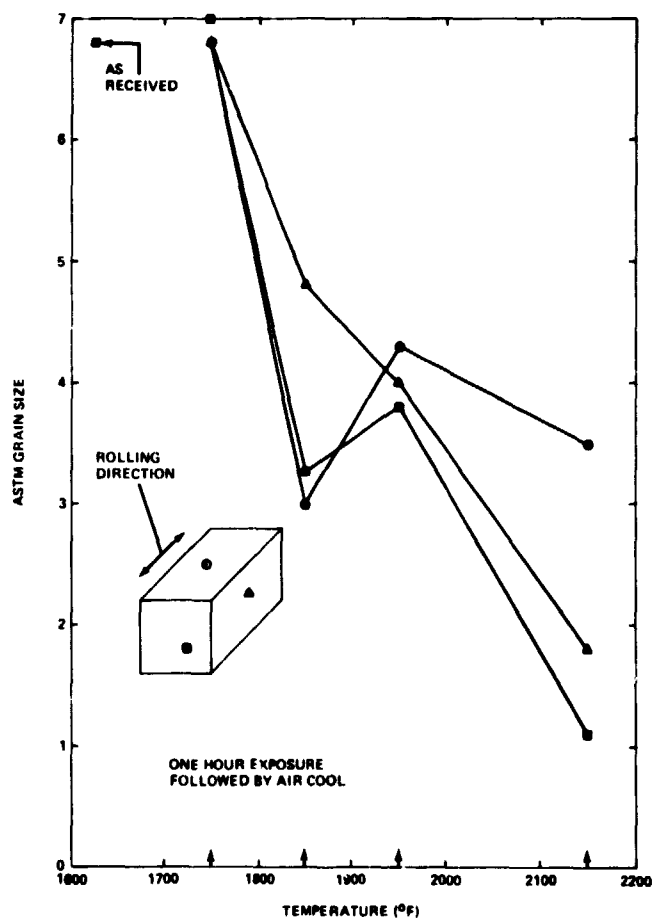
Large grains, produced at temperatures above 1825°F at which the grain-boundary-pinning delta phase dissolves, appear to be a necessary but not sufficient condition for microfissuring [8,9]. The effect of large grains could be to concentrate detrimental impurities in reduced grain boundary area. A simple mechanical explanation for the grain boundary effect on microfissuring, however, comprises a limited deformation capacity for a single grain boundary so that a strain concentrated at liquated grain boundaries becomes more potent the fewer the grain boundaries available to absorb it. The latter explanation is more attractive because of its simplicity and because it is easily quantified. As will be seen further in this report, the latter explanation, when quantified, appears to fit the data available at present.

It is possible to build not merely a plausible qualitative picture, but a rough quantitative model of the microfissuring process from the above clues and a physical understanding of the weld process. This has been accomplished and, pending further experimental study, the model appears to fit the experimental data and to offer predictive capability.

TEST PROCEDURE

Eight microfissuring specimens of 0.25-in. thick Inconel 718 plate were cut 4-in. wide by 12-in. long. Four of the plates were heat treated for 1 hr at 2150°F followed by an air cool.

The object in heat treating half the specimens was to make them more prone to microfissuring. Large grains appear to be associated with microfissuring. Figure 1 shows the results of grain size measurements taken on Inconel 718 samples exposed to 1750, 1850, 1950, and 2150°F for 1 hr followed by an air cool. An ASTM grain size of 6 or 7 is normal for as received wrought Inconel 718 plate. An ASTM grain size around 2 would be expected to result from the above heat treatment.



ORIGINAL PAGE IS
OF POOR QUALITY

Figure 1. Grain growth in Inconel 718 during 1 hr exposure to various temperatures followed by air cool to room temperature.

**ORIGINAL PAGE IS
OF POOR QUALITY**

An EB bead-on-plate weld was run down the center of each plate using the voltage/current/speed parameters listed in Table 1. As shown in Figure 2 closely equivalent weld profiles were obtained with some focus adjustment. A mean weld root of 0.099 in. with a standard deviation of 0.010 in. and a mean weld crown of 0.137 in. with a standard deviation of 0.005 in. were obtained. A tendency of the weld fusion metal to drop down below the plate surface was observed, most pronounced at the slowest speeds (specimens 4 and 8).

TABLE 1. WELDING PARAMETERS USED

Specimen No. ^a	Voltage (kV)	Current (mA)	Speed (IPM) ^b
1,5	140	40	40
2,6	140	30	30
3,7	140	20	20
4,8	140	10	10

- a. Specimens 1 through 4 were heat treated at 2150°F for 1 hr followed by an air cool. Specimens 5 through 8 were as received.
- b. In all cases the energy delivered was 8.4 kJ/in. An increase in current (power) was compensated by an increase in weld speed.

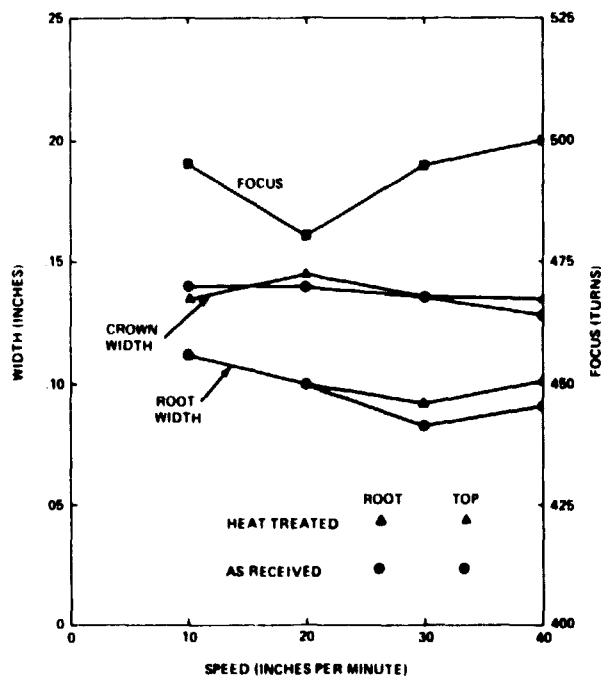


Figure 2. Crown and root widths of EB welds in 0.25-in. thick Inconel 718 plate made with the same energy per unit weld length but at different weld speed/power combinations. Focus adjustments needed to maintain approximately the same crown and root width are also shown.

The weld top surface was ground down 0.030 in. below the plate surface to reach the microfissured regions in steps of 0.010 in. The surface was etched [50 percent HCl-50 percent H_2O_2 (30 percent by volume)] after grinding. A fluorescent dye penetrant was then used to reveal the microfissures.

TEST RESULTS

Three of the four heat-treated specimens exhibited microfissures 0.030 in. below the top surface of the plate. The number of microfissures appeared to increase by roughly 2.25 microfissures per inch per kilowatt as shown in Figure 3.

No microfissures were exhibited by the four as-received plates, which were subjected to the same weld procedures as the heat-treated plates.

THEORY OF MICROFISSURING

Microfissuring is thought to take place due to the action of tensile strains in the weld HAZ during the period when the HAZ begins to cool down and contract while its environment continues to heat up and expand. The tensile strains result as the shrinking HAZ is forced to conform to its still expanding environment.

The mathematical model of microfissuring constructed here comprises three parts:

- 1) A model of the temperature field in the vicinity of the weld.
- 2) A computation of the stress-strain state in the vicinity of the weld due to the thermal stresses produced by the temperature field.
- 3) A criterion for formation of microfissures under the stress-strain conditions prevailing in the weld HAZ.

The model presented here employs only elementary components necessary to make an approximate calculation of the likelihood of observing microfissuring under a given weld situation. Experimental work is continuing to fully validate this model or an improved version. Improvements in the model are feasible and may turn out to be necessary in the light of future experimental data.

The temperature field around the weld is modeled by an adaptation of the Rosenthal moving heat source model [10]. A moving point source on the surface of a plate of finite, specified width is combined with a moving line source extending down from the point source through the plate. The line source represents the spike of an EB weld; the point source, the nailhead, i.e., the extended region at the top of the weld, conceived as due to lower power density edge portions of the electron beam which fail to penetrate deeply and are absorbed at the top of the weld.

The temperature rise $T - T_0$ above ambient temperature T_0 due to a point source of power P_1 moving over the surface of the plate in the X-direction with velocity V is given by:

ORIGINAL PAGE IS
OF POOR QUALITY

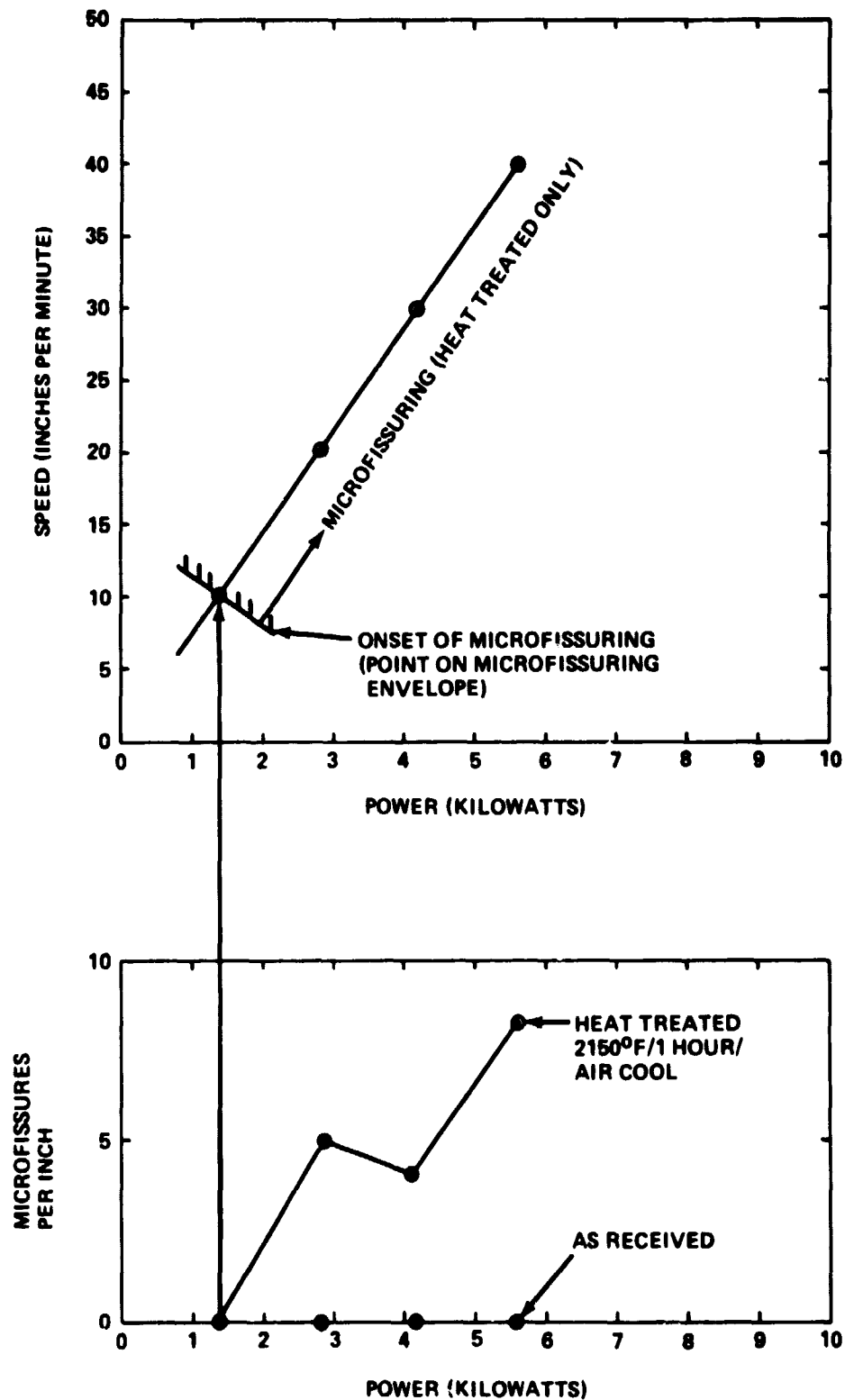


Figure 3. Microfissures per inch versus beam power and approximate location of microfissuring envelope point on speed/power constant weld cross section line.

$$T - T_o = \frac{P_1}{2\pi k} \left[\frac{e^{-\frac{V}{2\alpha}(r+x)}}{r} + \sum_{n=1}^{\infty} \left(\frac{e^{-\frac{V}{2\alpha}(r_n+x)}}{r_n} + \frac{e^{-\frac{V}{2\alpha}(r'_n+x)}}{r'_n} \right) \right] \quad (1)$$

where

k = thermal conductivity of metal

α = thermal diffusivity of metal

$$r_n = \sqrt{x^2 + y^2 + (z - 2nd)^2}$$

$$r'_n = \sqrt{x^2 + y^2 + (z + 2nd)^2}$$

x, y, z = location of temperature site with respect to point source at 0,0,0. x is in the direction of motion; y is directed to the side; and z , is directed down into the interior of the plate perpendicular to the plate surface

d = plate thickness.

The summation, which is, of course, truncated in the computer calculation, comprises image sources which produce the effect of the back surface of the plate.

The temperature rise $T - T_o$ above ambient due to a moving line source of total power P_2 distributed over the plate thickness d is given by:

$$T - T_o = \frac{P_2}{2\pi k d} e^{-\frac{V}{2\alpha}x} K_o \left(\frac{V}{2\alpha} R \right) \quad (2)$$

where

$$R = \sqrt{x^2 + y^2}$$

K_o = zero order modified Bessel function of the second kind.

An EB weld can be characterized by specifying P_1 and P_2 . In this work two "loss" parameters are used: F_1 , the overall loss parameter, given as a percent and defined such that

$$P_1 + P_2 = \left(1 - \frac{F_1}{100} \right) P_o \quad (3)$$

where P_0 = total beam power; and F_2 , the nailhead loss parameter, given as a percent and defined such that

$$P_1 = \frac{F_1}{100} \cdot (P_1 + P_2) \quad \text{ORIGINAL PAGE IS OF POOR QUALITY} \quad (4)$$

These losses can be calculated by matching the crown and root widths of a weld with the computed maximum widths between the solidus temperature isotherms at the top and bottom of the weld. The results of such calculations for the experimental welds of this report are shown in Figure 4.

The difficulties in calculating the stress-strain history in the weld HAZ were circumvented by a crude but highly simplifying approximation. The strain imposed upon the weld HAZ is assumed equal to the net difference in thermal expansion

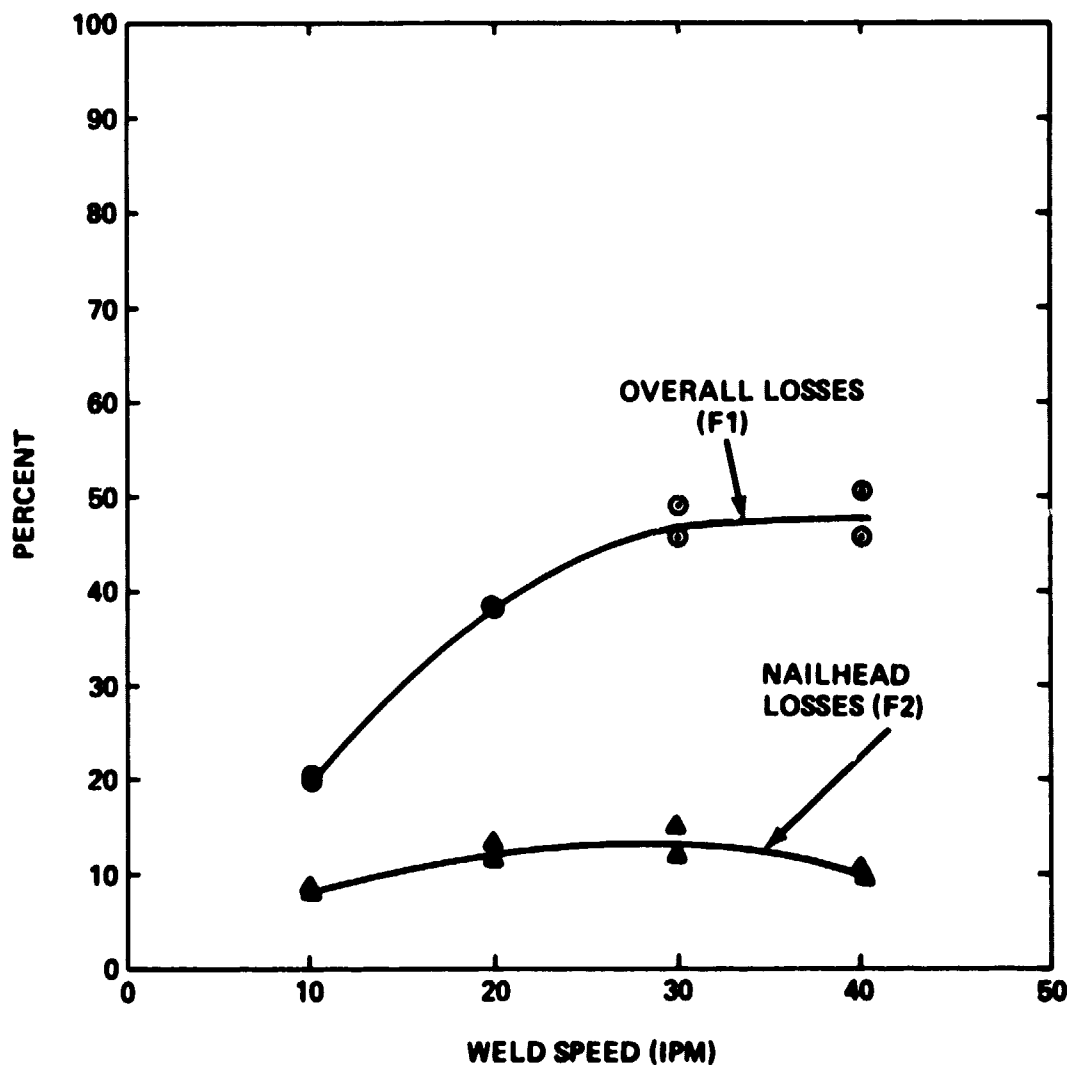


Figure 4. Overall and nailhead power losses versus weld speed for constant energy per length equivalent profile EB welds.

ORIGINAL PAGE IS
OF POOR QUALITY

between the HAZ itself and its "environment." The "environment" is tentatively assigned the temperature encountered at a distance twice as far out from the weld centerline as the width of the weld. Thus given thermal expansion coefficient μ , strain increment $\Delta \epsilon$ is encountered such that

$$\Delta \epsilon = \mu (\Delta T_e - \Delta T_{HAZ}) \quad (5)$$

where

ΔT_e = environmental temperature increment

ΔT_{HAZ} = HAZ temperature increment, as one moves from initially unstrained material back along the weld in the HAZ.

If no plastic strain were to occur the strain increment would be accompanied by a stress increment $\Delta \sigma$, where

$$\Delta \sigma = E \Delta \epsilon \quad (6)$$

where E = the linear elastic modulus of the metal. The use of a simple linear stress-strain relation is believed justified partly by the presence of molten or very soft material in the fusion zone of the weld preventing triaxial stress conditions during the imposition of a significant part of the thermal straining and partly by the inherent level of approximation which would make greater precision of one isolated aspect of the stress calculation superfluous.

A nominal stress σ_N is calculated by adding $\Delta \sigma$ to its initial value σ .

$$\sigma_N = \sigma + \Delta \sigma \quad (7)$$

and compared with an estimated flow stress σ_f , which vanishes at the metal melting point,

$$\sigma_f = K_s (T_M - T_{HAZ})^2 \quad (8)$$

where

K_s = constant

T_M = melting (solidus) temperature of metal

T_{HAZ} = HAZ temperature.

If the nominal stress σ_N would go outside the elastic region $-\sigma_f < \sigma_n < +\sigma_f$, then a plastic strain increment $\Delta \epsilon_p$ is computed sufficient to relax the nominal strain to a value that can be supported by the material. Thus, if

$$\sigma_N > \sigma_f ,$$

then

$$\Delta \epsilon_p = \Delta \epsilon \cdot \left[1 - \left(\frac{\sigma_f - \sigma}{\Delta \sigma} \right) \right] , \quad (9)$$

and a new stress is computed

$$\sigma = \sigma_f . \quad (10)$$

If $\sigma_N < -\sigma_f$, then

$$\Delta \epsilon_p = \Delta \epsilon \cdot \left[1 + \left(\frac{\sigma_f + \sigma}{\Delta \sigma} \right) \right] , \quad (11)$$

and

$$\sigma = -\sigma_f . \quad (12)$$

Otherwise,

$$\Delta \epsilon_p = 0 , \quad (13)$$

and

$$\sigma = \sigma_N .$$

Lastly, a damage theory of microfissuring is invoked, i.e., microfissuring is assumed to occur when

$$\sum \frac{\Delta \epsilon_p}{\epsilon_c} = 1 \quad (14)$$

where $\Delta \epsilon_p / \epsilon_c$ is the ratio of plastic strain increment to the critical plastic strain that would cause fracture under conditions of fixed temperature. Each plastic strain increment is assumed to contribute to the final fracture condition in proportion to its ratio to the critical fracture strain. This assumption must be regarded as tentative and subject to revision as further data is acquired. The precedent for use of a damage concept comes from fatigue research. As in the case of fatigue there is no reason to use a linear damage criterion except for simplicity's sake in the absence of experimental or theoretical justification for a more complex damage relation.

A critical fracture stress relation of the form

$$\epsilon_c = \epsilon_{co} \cdot e^{\frac{(T-T_G)^2}{B}} \cdot 2^{\left(\frac{GS-4}{2}\right)} \quad (15)$$

where ϵ_{co} , T_G , B are constants, and GS = grain size of metal, is assumed.

R. G. Thompson's plot [11,12] of temperature versus critical strain for a hot tensile test of Inconel 718 with an ASTM grain size of 4 supplied values for the constants:

$$\epsilon_{co} = 0.002$$

$$T_G = T_M - 25^\circ\text{F}$$

$$B = 2058 (\text{°F})^2$$

The grain size dependence assumes that a given extension per grain boundary Δd_G is required for fracture. If the grain diameter is d_G then

$$\frac{(\epsilon_{co})_{GS}}{(\epsilon_{co})_{GS=4}} = \frac{\left(\frac{\Delta d_G}{d_G}\right)_{GS}}{\left(\frac{\Delta d_G}{d_G}\right)_{GS=4}} = \frac{\left(\frac{1}{d_G}\right)_{GS}}{\left(\frac{1}{d_G}\right)_{GS=4}} \quad (16)$$

By definition the number of grains per square inch at a magnification of $\times 100$ is 2^{GS-1} , so that

$$\left(\frac{1}{d_G}\right)^2 \approx 2^{GS-1} \times 10^{-4} \quad (17)$$

and

ORIGINAL PAGE IS
OF POOR QUALITY

$$\left(\frac{t_{co}}{t_{co}}\right)_{GS-4} = \frac{GS/2}{2^{4/2}} = 2^{\left(\frac{GS-4}{2}\right)} \quad (18)$$

This accounts for the grain size correction exhibited in equation (15).

These mathematical pieces have been put together in a computer model written out in Appendix I. The model computes damage curves versus speed or power for selected loss conditions. A damage value in excess of one implies microfissuring.

Let it be noted in conclusion that a more detailed model should also take into account a hysteresis effect due to time variation in grain boundary wetting. This has not been incorporated into the present model, nor is it likely to be until much more experimental data on the microfissuring process becomes available.

COMPARISON OF THEORY AND EXPERIMENT

With the assumptions incorporated into the theory of microfissuring presented here, it was anticipated that some adjustment of the model would be required to reach good agreement with empirical data. Nevertheless, at this point, theory and experiment appear to agree well.

Table 2 shows computer model predictions of power-speed combinations at which microfissuring begins. Table 3 shows the excess of power over that which should, according to the computer model, produce microfissuring. Where there is an excess of power, microfissuring would be expected. Where there is an insufficiency of power, microfissuring would not be expected.

TABLE 2. COMPUTER MODEL PREDICTIONS OF POWER SPEED COMBINATION AT WHICH MICROFISSURING BEGINS

Specimen No.	Estimated GS	Power (kW)	Speed (IPM)
1	2	1.7	7
2	2	1.7	7
3	2	1.2	6
4	2	1.1	6
5	6	a	a
6	6	a	a
7	6	a	a
8	6	a	a

a. Powers substantially above 30 kW and speeds substantially above 300 IPM would be required.

TABLE 3. EXCESS POWER ABOVE COMPUTER MODEL POWER
REQUIREMENT TO INITIATE MICROFISSURING

Specimen No.	Excess Power
1	+3.9
2	+2.5
3	+1.6
4	+0.3
5	a
6	a
7	a
8	a

a. Substantially negative excess power (>-25 kW) predicts no microfissuring.

Figure 5 is a plot of measured microfissures per inch versus calculated microfissuring power excess for the four heat-treated specimens. Microfissuring only occurred for these specimens, where there was a calculated excess power. From the limited data it would appear that the amount of microfissuring increases with excess power at approximately 4.5 microfissures per inch per excess kilowatt.

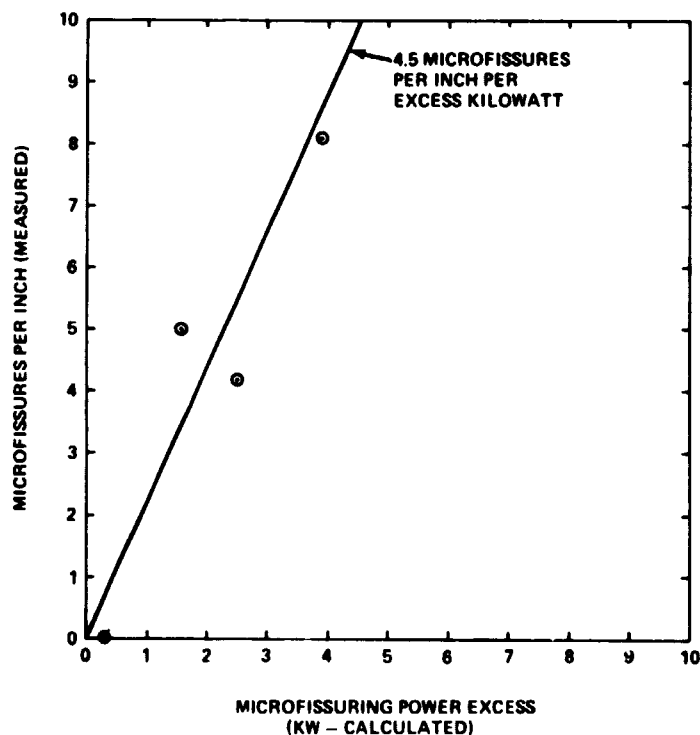


Figure 5. Microfissures per inch versus microfissuring power excess.

CONCLUSIONS AND RECOMMENDATIONS

Microfissures have been produced in 0.25-in. thick Inconel 718 plates by electron beam welding.

A computer model of microfissuring has been worked out. The model is compatible with the experimental data obtained so far. The power level required by the model to produce microfissuring can be computed for a given weld situation. About 4.5 microfissures per inch per excess kilowatt above the computed level to produce microfissuring were produced. Slowing the weld speed and reducing power below the level required to produce microfissures should eliminate microfissuring.

The model incorporates effects of weld power and speed, weld loss or efficiency parameters, and grain size. It can be adapted to other metals subject to microfissuring by altering material parameters.

Further empirical work, particularly on thicker plate at higher powers, is needed to provide a more substantial data base suitable for thorough evaluation of the model.

Once a means for producing microfissured and unmicrofissured, but otherwise similar, welds has been perfected, a study of the effect of microfissuring on mechanical properties can and should be carried out. Some mechanical testing using the specimens prepared in the previously cited study is now being planned.

Further editing of the computer program to improve style and efficiency is needed. It is planned to do this in the course of preparing this and other weld model programs for public distribution through the Computer Software Management and Information Center at the University of Georgia.

REFERENCES

1. Morrison, T. J., Shira, C. S., and Weissenberg, L. A.: The Influence of Minor Elements on Alloy 718 Weld Microfissuring. Effects of Minor Elements on the Weldability of High-Nickel Alloys. Proceedings of a Welding Research Council Symposium, Houston, Texas, October 3, 1967, pp. 47-67.
2. Nunes, A. C., Jr.: Microfissuring of Electron Beam Welds in Nickel Base Alloys. Report: NASA/ASEE Summer Faculty Research Fellowship Program, University of Alabama Contract NGT-01-002-099, August 11, 1978, pp. XIX 1-23.
3. Arata, Y., Terai, K., Nagai, H., Shimizu, S., and Aota, T.: Fundamental Studies on Electron Beam Welding of Heat-resistant Superalloys for Nuclear Plants (Report I). Transactions of JWRI, vol. 5, No. 2, 1976; reprinted in Welding Research Abroad, vol. 23, No. 6, June-July 1977, pp. 23-30.
4. Thompson, R. G.: On the Relationship Between Microfissuring and Microstructure in the HAZ of Inconel 718. Report: NASA/ASEE Summer Faculty Research Fellowship Program, The University of Alabama in Huntsville Contract No. NGT-008-021, August 27, 1981, pp. XXXV 1-22.
5. Thompson, R. G.: Further Study of Near Solidus Intergranular Hot Cracking in Inconel 718. Final Report: NASA Contract No. NAS8-33805, September 17, 1981.
6. Gordine, J.: Some Problems in Welding Inconel 718. Welding Journal, Research Supplement, vol. 50, No. 11, November 1971, pp. 480-S to 484-S.
7. Eidel'shtein, V. E., Yakushin, B. F., and Stolbov, V. I.: High Temperature Deformation and the Formation of Cracks in the Heat Affected Zone When Nimonic-Type Alloys are Welded. Avt. Svarka, No. 11, 32, 1976; translated in Automatic Welding, vol. 29, No. 11, November 1976, pp. 32-36.
8. Douty, R. A. and Schwarzbart, H.: Cobalt Base Surfacing of Inconel 718. Welding Journal, Research Supplement, vol. 52, No. 12, December 1973, pp. 550-S to 556-S.
9. Bologna, D. J.: Metallurgical Factors Influencing the Microfissuring of Alloy 718 Weldments. Metals Engineering Quarterly, vol. 9, No. 4, November 1969, pp. 37-43.
10. Rosenthal, D.: The Theory of Moving Sources of Heat and Its Application to Metal Treatments. Transactions of the American Society of Mechanical Engineers, vol. 68, November 1946, pp. 849-865, Discussion pp. 865-866.
11. Thompson, R. G.: Grain Boundary Hot Cracking in Inconel 718. Report: NASA/ASEE Summer Faculty Research Fellowship Program, The University of Alabama in Huntsville Contract No. NGT 01-008-021, August 11, 1979, pp. XXIX 1-28.
12. Thompson, R. G.: Hot Tensile Test of IN-718. Final Report: NASA Contract No. NAS8-33524, November 24, 1980.

APPENDIX A

MICROFISSURING MODEL COMPUTER PROGRAM LISTING

Overall and nailhead losses plus the desired weld root width are inserted into the program. A velocity range, usually 0 to 100 inches per minute, is preselected within the program but can be changed if desired.

The power settings corresponding to the velocities are computed as well as the location of the peak temperature position of the HAZ. Starting at the beginning of cool-off the plastic strain associated with the thermal stresses is estimated for a series of positions from the cool-off point to a point 2.5 in. behind the weld. A nonlinear scale weighted to take more points at higher temperatures is used.

From the difference between the estimated critical fracture strain (equation 15) and the plastic strain calculated as explained above is calculated a damage parameter, which is plotted versus power and velocity as program output. If the damage parameter exceeds unity, microfissuring is predicted.

The program is written in TEK SPS VO2-01 Basic for use on a Tektronix CP 1164 (DEC PDP 1134) central processor incorporated into a Tektronix WP 1220 Mod 04 Data Acquisition System. The program runs in a little over an hour.

```

10 REM *** MICROFISSURING DAMAGE CALCULATION ***
20 REM *** DATA INPUT ***
30 CLEAR
40 PRINT "PLEASE SELECT THE NUMBER OF THE METAL TO BE WELDED"
50 PRINT "FROM THE LIST BELOW." PRINT PRINT
60 PRINT "0 UNLISTED METAL" PRINT
70 PRINT "1 2219 ALUMINUM" PRINT
80 PRINT "2 302 STAINLESS STEEL" PRINT
90 PRINT "3 321 STAINLESS STEEL" PRINT
100 PRINT "4 INCONEL 718" PRINT
110 INPUT Q
120 IF Q=1 THEN 460
130 IF Q=2 THEN 490
140 IF Q=3 THEN 520
150 IF Q=4 THEN 550
160 PRINT "WHAT IS THE METAL TO BE WELDED?" PRINT PRINT PRINT
170 INPUT M$
180 PRINT "PLEASE WRITE IN THE LOWER AND UPPER LIMITS OF THE MELTING"
190 PRINT "TEMPERATURE RANGE OF THE ALLOY TO BE WELDED. USE UNITS OF"
200 PRINT "DEGREES FAHRENHEIT SEPARATE THE TWO VALUES BY A COMMA."
210 PRINT "NOTE: A GOOD SOURCE REFERENCE FOR THIS KIND OF DATA IS THE"
220 PRINT "AEROSPACE STRUCTURAL MATERIALS HANDBOOK." PRINT PRINT PRINT
230 INPUT LT,UT
240 PRINT "WHAT IS THE THERMAL CONDUCTIVITY OF THE ALLOY IN BTU'S PER"
250 PRINT "HOUR PER FOOT PER DEGREE FAHRENHEIT?" PRINT PRINT PRINT
260 INPUT K1
270 LET K1=K1*2.441E-05
280 PRINT "WHAT IS THE SPECIFIC HEAT OF THE ALLOY IN BTU'S PER LB"
290 PRINT "PER DEGREE FAHRENHEIT?" PRINT PRINT PRINT
300 INPUT C1
310 PRINT "WHAT IS THE DENSITY OF THE ALLOY IN LBS PER CUBIC INCH?"
320 PRINT PRINT PRINT
330 INPUT R0
340 LET A1=K1/R0/C1*56.83

```

ORIGINAL PAGE IS
DE POOR QUALITY

```

350 PRINT "WHAT IS THE COEFFICIENT OF THERMAL EXPANSION "
360 PRINT "IN INCHES PER INCH PER DEGREE FAHRENHEIT?"
370 INPUT MU
380 PRINT "WHAT IS THE ELASTIC MODULUS IN PSI?"
390 INPUT E
400 PRINT "ASSUMING THAT, IN THE NEIGHBORHOOD OF MELTING, THE"
410 PRINT "FLOW STRESS IS PROPORTIONAL TO THE SQUARE OF THE "
420 PRINT "DIFFERENCE BETWEEN HAZ TEMPERATURE AND MELTING "
430 PRINT "TEMPERATURE, WHAT IS THE FLOW STRESS COEFFICIENT"
440 PRINT "IN PSI PER DEGREES FAHRENHEIT SQUARED?"
450 INPUT KS
460 LET UT=1190\LET LT=1810\LET K1=2.44E-03\LET A1=.56
470 LET MU=1.44E-05\LET E=5000000\LET KS=.08
480 LET M$="2219 ALUMINUM"\GOTO 500
490 LET UT=2650\LET LT=2550\LET K1=4.27E-04\LET A1=.5
500 LET MU=1.2E-05\LET E=1.6E+07\LET KS=.05
510 LET M$="302 STAINLESS STEEL"\GOTO 500
520 LET UT=2550\LET LT=2500\LET K1=4.03E-04\LET A1=.66
530 LET MU=1.15E-05\LET E=1.6E+07\LET KS=.05
540 LET M$="321 STAINLESS STEEL"\GOTO 500
550 LET UT=2437\LET LT=2300\LET K1=3.83E-04\LET A1=.71
560 LET MU=9.0E-06\LET E=1.5E+07\LET KS=.056
570 LET M$="INCONEL 718"\GOTO 500
580 PRINT\PRINT\PRINT
590 PRINT "WHAT IS THE ASTM GRAIN SIZE OF THE METAL?"
600 PRINT\PRINT\PRINT
610 INPUT GS
620 PRINT "THE METAL TO BE WELDED IS NOW CHARACTERIZED. WE NOW"
630 PRINT "TURN TO THE WELDING PROCESS PARAMETERS." \PRINT\PRINT\PRINT
640 PRINT "WHAT IS THE AMBIENT TEMPERATURE OF THE METAL IN DEGREES"
650 PRINT "FAHRENHEIT? IF THE METAL IS PREHEATED, GIVE THE PREHEAT"
660 PRINT "TEMPERATURE AS THE AMBIENT TEMPERATURE." \PRINT\PRINT\PRINT
670 INPUT T0
680 PRINT "PLEASE SPECIFY THE PLATE THICKNESS IN INCHES."
690 PRINT\PRINT\PRINT
700 INPUT W1
710 PRINT "PLEASE SPECIFY WELD ROOT WIDTH IN INCHES. "
720 PRINT\PRINT\PRINT
730 INPUT WR
740 PRINT "WHAT PERCENT OF TOTAL BEAM POWER IS LOST FROM THE WELD"
750 PRINT "PUDDLE DUE TO PROCESSES OTHER THAN CONDUCTION BY THE PLATE?"
760 PRINT "THESE LOSSES INCLUDE RADIATION AND METAL EVAPORATION FROM"
770 PRINT "THE VICINITY OF THE PUDDLE." \PRINT\PRINT\PRINT
780 INPUT F1
790 PRINT "WHAT PERCENT OF THE REMAINING BEAM POWER IS ABSORBED CLOSE"
800 PRINT "TO THE METAL SURFACE SO AS TO FORM THE EB WELD NAILHEAD?"
810 PRINT "THIS WOULD BE THE PERCENTAGE OF THE BEAM CURRENT LACKING"
820 PRINT "SUFFICIENT POWER DENSITY TO VAPORIZE THE METAL."
830 PRINT\PRINT\PRINT
840 INPUT F2
850 PRINT "PLEASE SELECT POWER RANGE UPPER LIMIT IN KILOWATTS."
860 PRINT "5, 10, 25, OR 50."
870 INPUT KW
880 PRINT "TO PROCEED PRESS THE SPACE BAR "
890 WAIT
900 PAGE
910 ONERR NOWARN
920 REM *** CONSTANT PENETRATION LINE PLOT ***
930 DELETE UA,PA
940 LET M=20
950 DIM U$(M),PA$(M),XS(M)
960 LET UZ=100
970 FOR I=0 TO M
980 LET U$(I)=UZ*((I+1)/(M+1))
990 LET U1=U$(I)
1000 GOSUB 2340
1010 LET XS(I)=X
1020 LET PA$(I)=P0
1030 NEXT I
1040 DELETE PB,UB

```

ORIGINAL PAGE IS
OF POOR QUALITY

```

1050 DIM PB(M),UB(M)
1060 FOR I=0 TO M
1070 LET UB(I)=UA(I)
1080 LET PB(I)=PA(I)
1090 IF PA(I)<KW THEN 1130
1100 IF PA(I)>KW THEN IF PA(I-1)>KW THEN 1120
1110 LET UB(I)=UA(I-1)+(U2/(M+1))*((KW-PA(I-1))/(PA(I)-PA(I-1)))
1120 IF PA(I)>KW THEN LET PB(I)=KW
1130 NEXT I
1140 PAGE
1150 GOSUB 1690
1160 FOR I=0 TO 10\PRINT\NEXT I
1170 PRINT "WELD SPEED"
1180 PRINT " (IPM)"
1190 FOR I=0 TO 14\PRINT\NEXT I
1200 PRINT "                                BEAM POWER (KILOWATTS)"
1210 WINDOW 0,KW,0,U2
1220 VIEWPORT 260,763,156,650
1230 SETGR VIEW,WINDOW,TICS 10,10,5,5,GRAT 6,6,3,3
1240 XYPLOT PB,UB
1250 PRINT "A-W-E-L"
1260 DELETE DA
1270 DIM DA(M)
1280 FOR J=0 TO M
1290 LET P2=PA(J)*(1-F1/100)
1300 LET P1=P2*(F2/100)
1310 LET P2=P2-P1
1320 LET U1=UA(J)
1330 GOSUB 1760
1340 LET DA(J)=DM
1350 NEXT J
1360 DELETE DB
1370 DIM DB(M)
1380 FOR I=0 TO M
1390 LET DB(I)=DA(I)
1400 IF DA(I)>=2 THEN LET DB(I)=2
1410 NEXT I
1420 PAGE
1430 GOSUB 1690
1440 FOR I=0 TO 10\PRINT\NEXT I
1450 PRINT "WELD SPEED"
1460 PRINT " (IPM)"
1470 FOR I=0 TO 14\PRINT\NEXT I
1480 PRINT "                                DAMAGE"
1490 WINDOW 0,2,0,U2
1500 VIEWPORT 260,763,156,650
1510 SETGR VIEW,WINDOW,TICS 10,10,5,5,GRAT 6,6,3,3
1520 XYPLOT DB,UB
1530 PRINT "A-W-E-L"
1540 GOSUB 1690
1550 FOR I=0 TO 10\PRINT\NEXT I
1560 PRINT "DAMAGE"
1570 FOR I=0 TO 15\PRINT\NEXT I
1580 PRINT "                                BEAM POWER (KILOWATTS)"
1590 WINDOW 0,KW,0,2
1600 VIEWPORT 260,763,156,650
1610 SETGR VIEW,WINDOW,TICS 10,10,5,5,GRAT 6,6,3,3
1620 XYPLOT PB,DB
1630 REM *** DELAY TO PREVENT SKIPPING PLOT ***
1640 FOR I=0 TO 1000
1650 LET B=EXP(-I)
1660 NEXT I
1670 PRINT "A-W-E-L"
1680 END
1690 REM *** CURVE LABEL SUBROUTINE ***
1700 PRINT M$,"--",
1710 PRINT "PLATE THICKNESS: ",W1," INCHES"
1720 PRINT "HAZ ",Y," INCHES OFF CTR. ",Z," INCHES DEPTH.  GS= ",GS
1730 PRINT F1,"% NONCONDUCTIVE LOSSES--",F2,"% TO NAILHEAD"
1740 PRINT WR," INCH ROOT WIDTH"

```

```

1750 RETURN
1760 REM *** DAMAGE CALCULATION SUBROUTINE ***
1770 REM *** COMPUTATION OF HAZ TEMPERATURE HISTORY ***
1780 LET Z=.03 REM DEPTH OF MICROFISSURING IS .030 INCHES
1790 GOSUB 2540
1800 DELETE XA,XB,TA,TB,TC,TD,S,EF,EP,ET
1810 LET N=200
1820 LET XF=2.5
1830 DIM XA(N),TA(N),TB(N),TC(N),TD(N)
1840 LET TA=UT LET TB=LT
1850 FOR I=0 TO N
1860 LET XA(I)=XS(J)*(XF-XS(J))*(I/N)*(I/N)
1870 LET X=-XA(I)
1880 GOSUB 2780
1890 LET TC(I)=M2
1900 LET Y1=Y
1910 LET Y=2*Y
1920 GOSUB 2780
1930 LET TD(I)=M2
1940 LET Y=Y1
1950 NEXT I
1960 REM *** COMPUTATION OF HAZ PLASTIC STRAIN HISTORY ***
1970 DIM S(N),EP(N)
1980 LET S=0 LET EP=0
1990 FOR I=1 TO N
2000 LET DE=MUX(TD(I)-TD(I-1)-TC(I)+TC(I-1))
2010 LET DS=EROE
2020 IF SQKDS<>SQKSI-1 THEN LET EP(I-1)=0
2030 IF (LT-TC(I))>0 THEN LET SF=KS*(LT-TC(I))/2
2040 IF (LT-TC(I))<0 THEN LET SF=0
2050 LET SN=SI-1+DS
2060 IF SN>SF THEN 2090
2070 IF SN<-SF THEN 2100
2080 IF SN<=SF THEN IF SN>=-SF THEN 2110
2090 LET EP(I)=EP(I-1)+DE*(1-(SF-SI-1)/DS) LET SI=SF GOTO 2120
2100 LET EP(I)=EP(I-1)+DE*(1-(SF+SI-1)/DS) LET SI=-SF GOTO 2120
2110 LET SI=SN
2120 NEXT I
2130 DIM ET(N)
2140 FOR I=0 TO N
2150 IF EP(I)>0 THEN LET ET(I)=EP(I)
2160 IF EP(I)<0 THEN LET ET(I)=0
2170 NEXT I
2180 REM *** FRACTURE ENVELOPE REPRESENTATION ***
2190 DIM EF(N)
2200 LET TG=LT-25
2210 FOR I=0 TO N
2220 LET EF(I)=2E-03*(2-((GS-4)/2))
2230 LET TF=(TC(I)-TG)*(TC(I)-TG)/2056
2240 IF TF>89 THEN LET TF=89
2250 LET EF(I)=EF(I)*EXP(TF)
2260 NEXT I
2270 REM *** DAMAGE CALCULATION ***
2280 LET DM=0
2290 FOR I=1 TO N
2300 IF EF(I)>9.99999E+34 THEN 2320
2310 IF ET(I)>ET(I-1) THEN DM=DM+(ET(I)-ET(I-1))/((EF(I)+EF(I-1))/2)
2320 NEXT I
2330 RETURN
2340 REM *** SUBROUTINE TO COMPUTE BEAM POWER ***
2350 LET Y=WR/2
2360 LET Z=w1
2370 LET T1=LT
2380 LET X=0
2390 LET DX=-.1
2400 LET P0=1
2410 LET P1=P0*(1-F1/100)
2420 LET P2=P1*(1-F2/100)
2430 LET P1=P1-P2
2440 GOSUB 2780

```


ORIGINAL PAGE IS
OF POOR QUALITY

```

2450 LET M4=M2
2460 LET X=X+DX
2470 GOSUB 2780
2480 LET M5=M2
2490 IF M5>M4 THEN GOTO 2450
2500 IF M5=M4 THEN GOTO 2520
2510 LET DX=(-DX)/10 GOTO 2450
2520 LET P0=P0*((T1-T0)/(M2-T0))
2530 RETURN
2540 REM *** LOCATION OF HEAT-AFFECTED-ZONE ***
2550 LET Y=.1 GOSUB 2670
2560 LET DY=.1
2570 LET M6=M2
2580 LET Y=Y+DY
2590 GOSUB 2670
2600 IF ABS(M2-LT)*.01<LT THEN 2660
2610 IF M2<LT THEN IF M6<M2 THEN 2570
2620 IF M2>LT THEN IF M6>M2 THEN 2570
2630 IF M2<LT THEN IF M6>M2 THEN LET DY=(-DY)/10
2640 IF M2>LT THEN IF M6<M2 THEN LET DY=(-DY)/10
2650 GOTO 2570
2660 RETURN
2670 REM *** TEMPERATURE MAXIMIZATION SUBROUTINE ***
2680 LET X=0
2690 LET DX=-.1
2700 GOSUB 2780
2710 LET M4=M2
2720 LET X=X+DX
2730 GOSUB 2780
2740 IF M4<M2 THEN 2710
2750 IF M4=M2 THEN 2770
2760 LET DX=-DX/10 GOTO 2710
2770 RETURN
2780 REM *** SUBROUTINE TO COMPUTE TEMPERATURE OF HEAT SOURCE ARRAY ***
2790 LET Z2=Z

```

```

2800 LET M2=0
2810 LET D3=0
2820 LET D2=2*M1
2830 GOSUB 3170
2840 GOSUB 3000
2850 LET M2=M1+T0+T2
2860 LET M3=M2
2870 LET D3=D3+D2
2880 GOSUB 2920
2890 IF (M2-M3)*.01<M2 THEN GOTO 2910
2900 GOTO 2860
2910 RETURN
2920 REM *** SUBROUTINE TO ADD NEXT TWO HEAT SOURCES ***
2930 LET Z2=D3+Z
2940 GOSUB 3170
2950 LET M2=M2+M1
2960 LET Z2=D3-Z
2970 GOSUB 3170
2980 LET M2=M2+M1
2990 RETURN
3000 REM *** SUBROUTINE TO COMPUTE LINE HEAT SOURCE TEMPERATURE
3010 REM DISTRIBUTION ***
3020 LET K0=0
3030 LET T2=0
3040 LET AP=U1/2/A1*X
3050 LET Z3=U1/2/A1*SGN(X*X+Y*Y)
3060 IF AP/88 THEN 3160
3070 GOSUB 3250
3080 IF AP<0 THEN 3110
3090 LET T2=P2/W1/6.2832/K1/EXP(AP)*K0
3100 GOTO 3160
3110 LET AR=-AR
3120 IF Z3>20 THEN 3150
3130 LET T2=P2/W1/6.2832/K1*EXP(AR)*K0
3140 GOTO 3160

```

```

3150 LET T2=P2/W1/6.2832/K1*1.2533/EXP(Z3-AR)/SQR(Z3)
3160 RETURN
3170 REM *** SUBROUTINE TO COMPUTE TEMPERATURE ***
3180 LET S1=SQR(X*X+Y*Y+Z2*Z2)
3190 IF S1=0 THEN LET M1=UT+1000\IF S1=0 THEN 3240
3200 LET AR=V1/2/A1*(S1+X)
3210 IF AR>88 THEN LET M1=0
3220 IF AR>88 THEN GOTO 3240
3230 LET M1=P1/2/3.1416/K1/S1/EXP(AR)
3240 RETURN
3250 REM *** MODIFIED BESSEL FUNCTION, SECOND KIND, ZEROth ORDER ***
3260 REM *** POLYNOMIAL APPROXIMATION ***
3270 IF Z3>88 THEN 3400
3280 IF Z3>2 THEN 3350
3290 GOSUB 3420
3300 LET G2=Z3*Z3/4
3310 LET K0=((7.4E-06*G2+1.075E-04)*G2+2.62698E-03)*G2
3320 LET K0=((K0+0.348859)*G2+2.386976)*G2
3330 LET K0=((K0+4.227842)*G2-5.772157)-5*LOG(G2)*I0
3340 GOTO 3410
3350 LET G2=2/Z3
3360 LET K0=((5.3208E-04*G2-2.5154E-03)*G2+5.87872E-03)*G2
3370 LET K0=((K0-0.1062446)*G2+0.2189568)*G2
3380 LET K0=((K0-0.7832358)*G2+1.253314)/SQR(Z3)/EXP(Z3)
3390 GOTO 3410
3400 LET K0=0
3410 RETURN
3420 REM *** MODIFIED BESSEL FUNCTION, FIRST KIND, ZEROth ORDER ***
3430 REM *** POLYNOMIAL APPROXIMATION ***
3440 IF Z3>3.75 THEN 3500
3450 LET G1=Z3*Z3
3460 LET I0=((5.923979E-10*G1+6.56017E-08)*G1+6.88123E-06)*G1
3470 LET I0=((I0+4.3394E-04)*G1+0.156252)*G1
3480 LET I0=((I0+0.25)*G1+1
3490 GOTO 3540
3500 LET I0=((153.445/Z3-171.822)/Z3+73.2919)/Z3
3510 LET I0=((10-15.2595)/Z3+1.81198)/Z3
3520 LET I0=((10-8838909)/Z3+0.316855)/Z3
3530 LET I0=((10+0.498222)/Z3+0.3989423)*EXP(Z3)/SQR(Z3)
3540 RETURN

```

READY
*

ORIGINAL PAGE IS
OF POOR QUALITY

APPENDIX B

SAMPLE MICROFISSURING MODEL OUTPUT

The microfissuring model computer program prints:

- 1) A curve of weld speed versus beam power for the assumed loss parameters.
- 2) A curve of damage versus beam power.
- 3) A curve of weld speed versus damage.

The weld speeds and beam powers for which the damage exceeds unity are taken to exhibit microfissuring.

INCONEL 718--PLATE THICKNESS: .25 INCHES
MAC .056 INCHES OFF CTR .25 INCHES DEPTH GS= 2
20.5% NONCONDUCTIVE LOSSES-- 7.5% TO NAILHEAD
112 INCH ROOT WIDTH

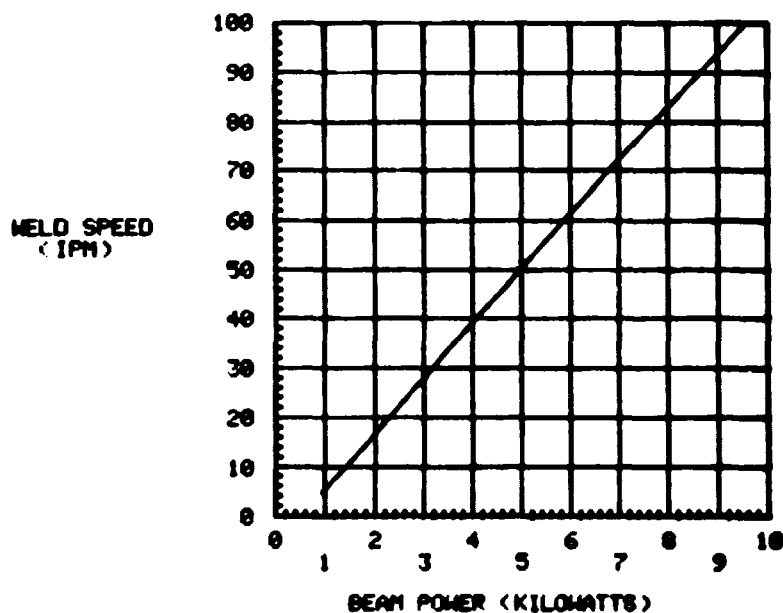


Figure 6. Computer output: weld speed versus beam power.

INCONEL 718--PLATE THICKNESS .25 INCHES
HAZ .069 INCHES OFF CTR. .03 INCHES DEPTH. GS= 2
20.5% NONCONDUCTIVE LOSSES-- 7.5% TO NAILHEAD
.112 INCH ROOT WIDTH

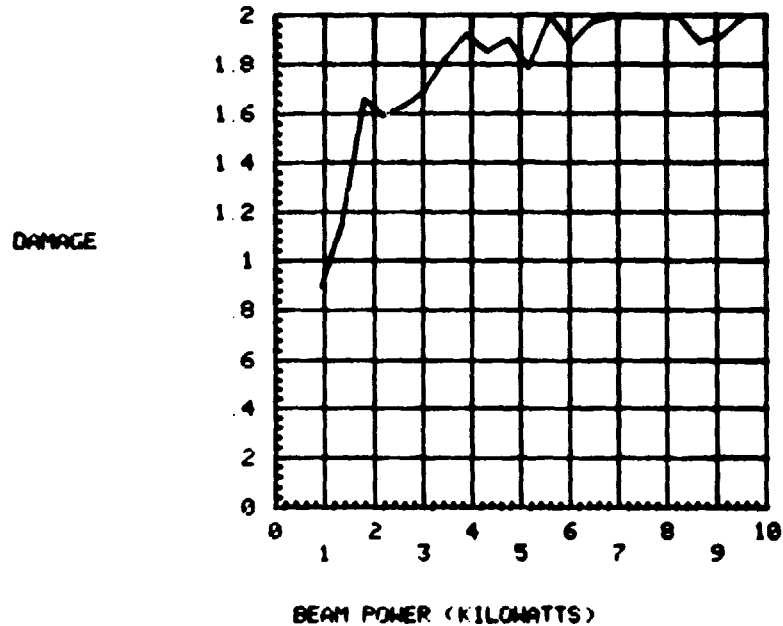


Figure 7. Computer output: damage versus beam power.

INCONEL 718--PLATE THICKNESS .25 INCHES
HAZ .069 INCHES OFF CTR. .03 INCHES DEPTH. GS= 2
20.5% NONCONDUCTIVE LOSSES-- 7.5% TO NAILHEAD
.112 INCH ROOT WIDTH

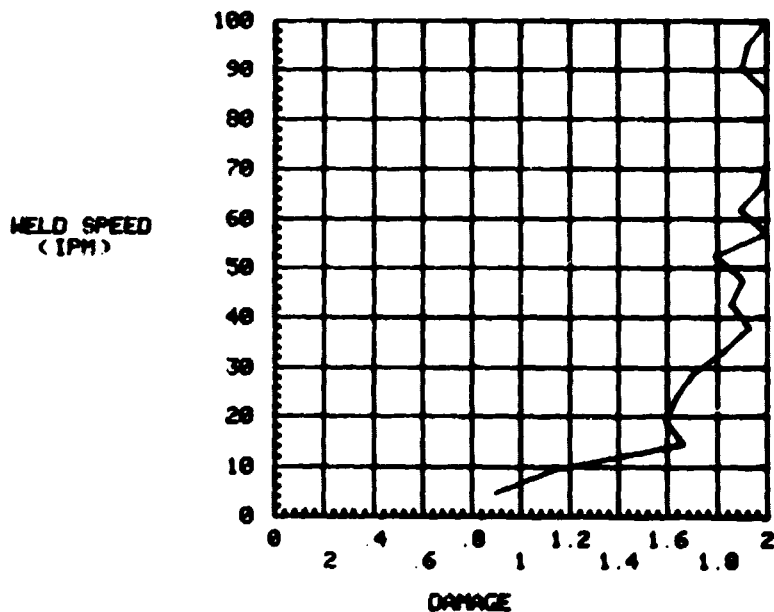


Figure 8. Computer output: weld speed versus damage.


APPROVAL

ORIGINAL PAGE IS
OF POOR QUALITY

INTERIM REPORT ON MICROFISSURING OF INCONEL 718

By A. C. Nunes, Jr.

The information in this report has been reviewed for technical content. Review of any information concerning Department of Defense or nuclear energy activities or programs has been made by the MSFC Security Classification Officer. This report, in its entirety, has been determined to be unclassified.



R. J. SCHWINGHAMER
Director, Materials and Processes Laboratory